Medical Engineering & Physics 32 (2010) 1–6

Contents lists available at ScienceDirect

Medical Engineering & Physics

journal homepage: www.elsevier.com/locate/medengphy

Development of a new method for the noninvasive measurement of deep body temperature without a heater

Kei-Ichiro Kitamura[a,*], Xin Zhu[b], Wenxi Chen[b], Tetsu Nemoto[a]

[a] Department of Clinical Laboratory Science, Division of Health Sciences, Graduate School of Medical Science, Kanazawa University, 5-11-80 Kodatsuno, Kanazawa, Ishikawa 920-0942, Japan
[b] Biomedical Information Technology Laboratory, Graduate School of Computer Science and Engineering, the University of Aizu, Aizu-Wakamatsu, Fukushima 965-8580, Japan

ARTICLE INFO

Article history:
Received 8 July 2009
Received in revised form
17 September 2009
Accepted 20 September 2009

Keywords:
Transcutaneous deep body temperature
Non-heating
Battery driven

ABSTRACT

The conventional zero-heat-flow thermometer, which measures the deep body temperature from the skin surface, is widely used at present. However, this thermometer requires considerable electricity to power the electric heater that compensates for heat loss from the probe; thus, AC power is indispensable for its use. Therefore, this conventional thermometer is inconvenient for unconstrained monitoring. We have developed a new dual-heat-flux method that can measure the deep body temperature from the skin surface without a heater. Our method is convenient for unconstrained and long-term measurement because the instrument is driven by a battery and its design promotes energy conservation. Its probe consists of dual-heat-flow channels with different thermal resistances, and each heat-flow-channel has a pair of IC sensors attached on its top and bottom. The average deep body temperature measurements taken using both the dual-heat-flux and then the zero-heat-flow thermometers from the foreheads of 17 healthy subjects were 37.08 °C and 37.02 °C, respectively. In addition, the correlation coefficient between the values obtained by the 2 methods was 0.970 ($p < 0.001$). These results show that our method can be used for monitoring the deep body temperature as accurately as the conventional method, and it overcomes the disadvantage of the necessity of AC power supply.

1. Introduction

Core body temperature is the deep body temperature of the internal organs in the abdominal, thoracic, and cranial cavities. Core body temperature shows individual physiological states that contribute to its variability, including the metabolic rate (the rate at which the body consumes energy while at that point), physical conditions such as menstruation, and the ingestion of various medications. Therefore, the measurement of core body temperature has been thought to assume greater significance in the care of seriously ill patients who cannot comment about their own physical conditions. This is particularly the case in the management of hypothermia, in paediatrics, and in anaesthesia [1–5].

The method generally used for the measurement of human core body temperature involves the direct insertion of a sensor into a natural body cavity such as the rectum. However, the human body does not have such suitable cavities in which the thermal sensor can be inserted to measure the core temperature satisfactorily over a long time period, especially in subjects that are awake. Furthermore, these measurements in a body cavity can cause complications such as tympanic membrane perforation during general anaesthesia [6,7]. Another example of the complications that can arise while measuring the core body temperature is the risk of perforation of the rectum by the probe, especially in children [8]. In order to avoid these problems related to temperature measurement, the indirect measurement of the deep body temperature from the skin surface has been considered desirable. However, the measurement of the thermal resistance values of the skin and the subcutaneous tissue is difficult. Moreover, the thermal resistance value differs according to the part of the body, even in the same subject, and is strongly influenced by the blood flow at a particular time point [9].

In 1971, Fox and Solman [10,11] introduced a novel noninvasive technique for the measurement of the deep body temperature using the zero-heat-flow method. Their method provides an isothermal zone by using an electronic servocontrolled heater to prevent the heat loss by outflow. Although this technique is now widely used for monitoring the deep body temperature in cardiac surgery and intensive care units [12,13], this heating method requires a considerable amount of electric power. Therefore, the AC power supply is indispensable for this method of thermometry, which makes this method inconvenient for unconstrained monitoring. We have

* Corresponding author. Tel.: +81 76 265 2595; fax: +81 76 234 4369.
E-mail address: kkitamur@mhs.mp.kanazawa-u.ac.jp (K. Kitamura).

1350-4533/$ – see front matter © 2009 IPEM. Published by Elsevier Ltd. All rights reserved.
doi:10.1016/j.medengphy.2009.09.004

developed a new dual-heat-flux method using simplified heat flow simultaneous equations in thermal insulators with two different thermal resistance values. A new method described herein, allows for the indirect measurement of deep body temperature from the skin surface without the need for a heater to compensate for heat loss; we evaluated the measurement performance of this method by comparing the results with the conventional zero-heat-flow method.

2. Materials and methods

2.1. Principle of measurement

As shown in Fig. 1(a), when the body surface is covered with a thermal insulator and the temperature reaches equilibrium, the 2 heat flows—1 flow from the deep body tissue to the body surface beneath the thermal insulator and the other flow through the thermal insulator—are balanced. We assumed that there is a constant and vertical heat flow from the deep body to the surface of the thermal insulator. Therefore, when the thermal equilibrium is attained in the thermal insulator and the subcutaneous tissue, the heat flow can be calculated using the thermal resistance value of the thermal insulator and the temperatures at the 2 ends of the thermal insulator. The heat flow I is obtained by the following equation in the equivalent circuit illustrated in Fig. 1(b):

$$I = \frac{T_S - T_U}{R_I} \tag{1}$$

where T_S and T_U are temperatures at the skin beneath the insulator and at the top surface of the insulator, respectively, and R_I is the thermal resistance of the thermal insulator. Similarly, the heat flow I can also be determined from the deep body temperature beneath the insulator, the skin temperature, and the thermal resistance of the skin and hypodermic tissue. Then, the heat flow I can also be obtained by the following equation:

$$I = \frac{T_B - T_S}{R_S} \tag{2}$$

where T_B is the deep body temperature and R_S is the thermal resistance of the skin and subcutaneous tissue. Then, we can combine Eqs. (1) and (2) as follows:

$$I = \frac{T_S - T_U}{R_I} = \frac{T_B - T_S}{R_S} \tag{3}$$

Therefore, the deep body temperature can be obtained by modifying Eq. (3):

$$T_B = T_S + \frac{(T_S - T_U)R_S}{R_I} \tag{4}$$

However, the thermal resistance value R_S of the tissue beneath the insulator cannot be measured and is strongly influenced by the hypodermic blood flow at a particular time point.

When the body surface is covered with 2 closely placed thermal insulators with different thermal resistance values R_1 and R_2, as shown in Fig. 1(c), the deep temperature of each heat insulator can be obtained as follows:

$$\left.\begin{aligned} T_B &= T_1 + \frac{(T_1 - T_3)R_S}{R_1} \\ T_B &= T_2 + \frac{(T_2 - T_4)R_S}{R_2} \end{aligned}\right\} \tag{5}$$

where T_1 and T_2 are the skin temperatures beneath the 2 insulators, and T_3 and T_4 are the temperatures at the upper surface of the 2 insulators. Since the 2 insulators are placed close to each other, the thermal resistance R_S of the skin and subcutaneous tissue are nearly the same and can be eliminated from (5). We define the thermal resistance ratio R_1/R_2 as K; then, Eq. (5) can be rearranged as follows:

$$T_B = T_1 + \frac{(T_1 - T_2)(T_1 - T_3)}{K(T_2 - T_4) - (T_1 - T_2)} \tag{6}$$

When the ratio of the thermal resistance K is obtained, we can get the deep body temperature using Eq. (6).

As for the determination of K, we can modify Eq. (6) as follows:

$$K = \frac{(T_B - T_2)(T_1 - T_3)}{(T_B - T_1)(T_2 - T_4)} \tag{7}$$

In order to obtain the value of K, we conducted a simulation experiment in which we placed the probe containing the 2 insulators on a rubber sheet that was placed over the inner bottom of a copper vat floating in a water bath, and we then measured T_1, T_2, T_3, and T_4. Since the water temperature (T_B) in the simulation experiment was known, we could calculate the thermal resistance ratio K of the probe by using Eq. (7). Finally, the deep body temperature T_B can be calculated by the estimated K value using Eq. (6).

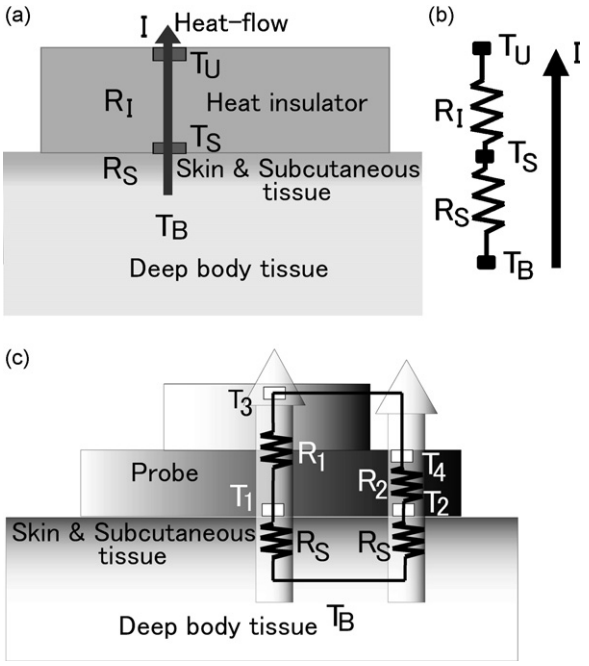

Fig. 1. Schematic diagrams of the heat flow and its equivalent circuits. (a) A schematic diagram of the heat flow when a part of the body surface is covered with the heat insulator. (b) A diagram of the equivalent circuit of (a), where the temperature, heat flow, and heat resistance correspond to the voltage, current, and resistance, respectively. (c) A schematic diagram of 2 channels of heat flow and its equivalent circuit, which is formed when the body surface is covered with 2 kinds of heat insulators with different thermal resistances R_1 and R_2. T_U, the temperature at the upper surface of the insulator; T_S, the temperature at the skin surface beneath the insulator; T_B, the deep body temperature; R_I, the thermal resistance of the insulator; R_S, the thermal resistance of the skin and subcutaneous fat; I, the heat current. T_1 and T_2 are the skin temperatures beneath the insulator, and T_3 and T_4 are the temperatures at the upper surface of the insulator.

2.2. Thermometer probe

Fig. 2(a)–(c) shows the thermometer probe, which is constructed using 4 integrated circuit (IC) temperature transducers (AD590, Analog Devices, Norwood, USA), a heat insulator, a copper disc, a copper ring, and a copper cap. The bottom of this probe contains the copper disc and the copper ring with good thermal conductivity, and they are directly placed on the body surface. Two ICs are placed at the bottom of the copper disc and the copper ring to monitor the skin temperatures T_1 and T_2. In addition, there are 2 ICs to monitor the temperatures T_3 and T_4 on the upper surface

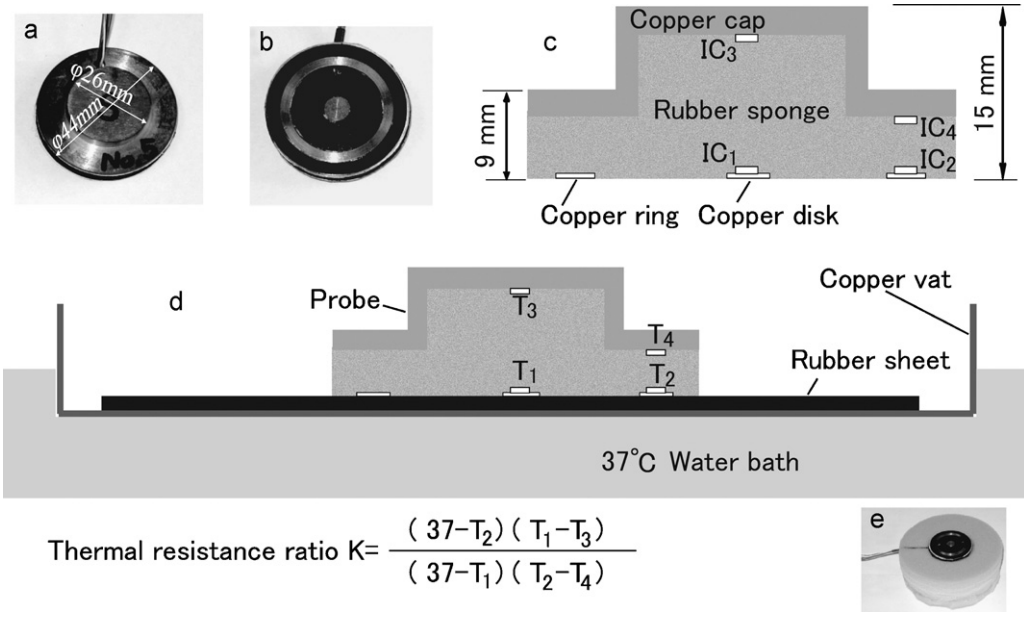

Fig. 2. The photographs and schemata of the probe of the dual-heat-flux thermometer and a simulation experiment. (a) The top view, (b) bottom view, and (c) lateral view of the probe. The bottom of the probe contains a copper disc and a copper ring with good thermal conductivity to be placed on the body surface. Two ICs are present on the copper disc and copper ring for measuring the skin temperatures T_1 (IC_1) and T_2 (IC_2). In addition, 2 other ICs are present under the copper cap of the probe for measuring the temperatures T_3 (IC_3) and T_4 (IC_4) at the upper surface. A heat insulator is present between the upper and lower ICs in the probe. IC_1, IC_3, and the heat insulator between them form a central heat flow channel. Similarly, IC_2, IC_4, and the heat insulator between them form a lateral heat flow channel. In the simulation experiment of the deep body temperature measurement (d), a copper vat was floated on the water bath at 37 °C, and a rubber sheet with a thermal conductivity (0.17 W m^{-1} K^{-1}) similar to that of the subcutaneous tissue was spread over the inner bottom surface of the vat. The water whose temperature is strictly controlled at 37.00 °C corresponds to a well-perfused deep body tissue, and the rubber sheet corresponds to the skin and subcutaneous tissue, where the thermal gradient is formed. The probe was applied on the rubber sheet, and T_1, T_2, T_3, T_4, and the water temperature were continuously monitored. (e) A photograph of the probe with a urethane sponge cover.

under the probe's copper cap. Heat insulators are present between the upper (IC_1 and IC_2) and lower temperature transducers (IC_3 and IC_4). IC_1, IC_3, and the heat insulator between them constitute a primary heat flow channel. Similarly, IC_2, IC_4, and the heat insulator between them constitute a secondary heat flow channel. The diameter, height, and weight of the probe are 44 mm, 15 mm, and 40 g, respectively.

2.3. Measurement of the K value in the simulation experiment

In the present study, the simulation experiment was conducted as according to the method of Nemoto and Togawa [14]. As shown in Fig. 2(d), the simulation system consisted of a water bath with a thermal controller, a copper vat, and a rubber sheet as a heat transfer layer. The copper vat was immersed in a thermostatically controlled water bath. The rubber sheet was placed on the bottom of the vat. Each rubber sheet was 1–10 mm thick with a thermal conductivity of 0.17 W m^{-1} K^{-1}. The water in the bath corresponding to the deep body tissue was strictly controlled at 37.00 °C by reference to a standard mercury-in-glass thermometer (Ando Keiki, Tokyo, Japan), which has markings from 33 °C to 43 °C at every 0.05 °C and with an accuracy of ±0.01 °C in the range of +33 °C to +42 °C. The rubber sheet corresponded to the epidermis and the subcutaneous tissue of the body, where the temperature gradient is produced. The probe was placed on the rubber sheet and T_1, T_2, T_3, and T_4 were continuously monitored; the measurement of the water temperature (T_B) was performed at the ambient temperatures of 20 °C, 25 °C, and 30 °C. An appropriate quantity of silicon grease was applied to the contact surfaces between the vat and the rubber sheet and between the rubber sheet and the probe to minimize the thermal boundary resistance. Moreover, in order to reduce the variance of the surface temperature of the probe due to the surrounding air current, the probe was covered with a urethane sponge, as illustrated in Fig. 2(e). After the thermal equilibrium was attained, we measured T_1, T_2, T_3, and T_4 and the water temperature (T_B). Through the measurements of these temperatures under different conditions and substitution of the corresponding variables in Eq. (7) with these measured values, the K values corresponding to each thickness of the rubber sheet at each room temperature were obtained. Then, the estimated deep temperature of the water in each condition was calculated by using Eq. (6) and the estimated K value for evaluation.

2.4. Comparison of the step responses to rapid changes in the deep temperature between the new and reference methods

We investigated the step responses of the dual-heat-flux and zero-heat-flow thermometers to the rapid changes in the deep body temperature in the simulation experiment with a 2 mm thick rubber sheet. In the simulation experiment, the water in the bath was maintained at 37 °C, and after we confirmed that the system had attained thermal equilibrium, the water at 37 °C was heated to 39 °C in 10 min at an ambient temperature of 20 °C. In this condition, we continuously measured the temperature using the dual-heat-flux thermometer, the zero-heat-flow thermometer, and the mercury thermometer of the water bath.

2.5. Measurement of the deep body temperature in healthy subjects

The deep body temperature was measured by the sponge-covered dual-heat-flux thermometer and the zero-heat-flow thermometer (CTM-205, Termo, Tokyo, Japan) in 17 healthy young subjects (21.5 ± 0.6 years old). Each subject sat on a chair in an air-conditioned room at 25 °C. The probes of the zero-heat-flow and dual-heat-flux thermometer were fixed on the right and left ante-

rior temporal regions, respectively, with a hair band. Each subject provided a written informed consent before participation in this study, which was approved by the Kanazawa University Human Research Ethics Committee.

3. Results

3.1. Determination of the thermal resistance ratio K

Fig. 3(a) shows the thermal resistance ratio K of the probe for rubber sheets of varying thickness at the ambient temperatures of 20 °C, 25 °C, and 30 °C. The K value in the simulation experiment was negligibly influenced by the thickness of the rubber sheet, but it changed with the ambient temperature. The average K values over the rubber sheet thickness range of 1–10 mm were 2.5, 2.8, and 3.0 at the ambient temperatures of 20 °C, 25 °C, and 30 °C, respectively.

3.2. Measurement of deep water temperature using the estimated K value

As shown in Fig. 3(b), the deep body temperatures of the water were calculated by using the estimated K values in the simulation experiments. At each room temperature, the calculated deep body temperatures were within 0.1 °C from the set value (37.00 °C) for each rubber sheet thickness.

Our probe was observed to be sensitive to air flow in the simulation experiment (data not shown). When a slight air flow existed near the probe, the temperature measured by each thermal transducer, especially IC_3 and IC_4, fluctuated and the achievement of the final equilibrium was delayed. Thus, we covered the probe with a sponge to protect it from the effects of air flow. The average K value over the rubber sheet thickness range of 1–10 mm of the sponge-covered probe in the simulation experiment was 4.0 at an ambient temperature of 20 °C (Fig. 3(a)). The errors in the estimated deep temperatures of the water using the sponge-covered probe were less than 0.1 °C (Fig. 3(b)). In addition, the sponge cover reduced fluctuations in the measured temperature due to the air flow (data not shown).

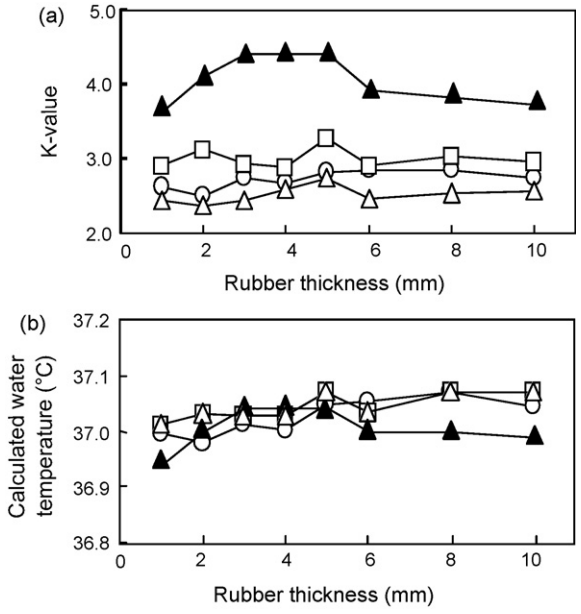

Fig. 3. The estimated thermal resistance ratio K in the simulation experiments (a) and the calculated deep temperatures of the water bath using the estimated K values corresponding to specified measurement conditions (b). The average K values for the rubber sheet thickness range of 1–10 mm were 2.5, 2.8, and 3.0 at ambient temperatures of 20 °C, 25 °C, and 30 °C, respectively. The estimated average K value over the rubber sheet thickness range of 1–10 mm of the sponge-covered probe in the simulation experiment was 4.0 at an ambient temperature of 20 °C. The error in the calculated water temperature from the set value (37.00 °C) was less than 0.1 °C for each rubber sheet thickness and each ambient temperature. The open triangle △ indicates the calculated K value in the upper panel (a) and the temperature in the lower panel (b) at an ambient temperature of 20 °C. The open circle ○ indicates the calculated K value in the upper panel (a) and the temperature in the lower panel (b) at an ambient temperature of 25 °C. The open square □ indicates the calculated K value in the upper panel (a) and the temperature in the lower panel (b) at an ambient temperature of 30 °C. The closed triangle ▲ indicates the calculated K value in the upper panel (a) and the temperature in the lower panel (b) on using the sponge-covered probe at an ambient temperature of 20 °C.

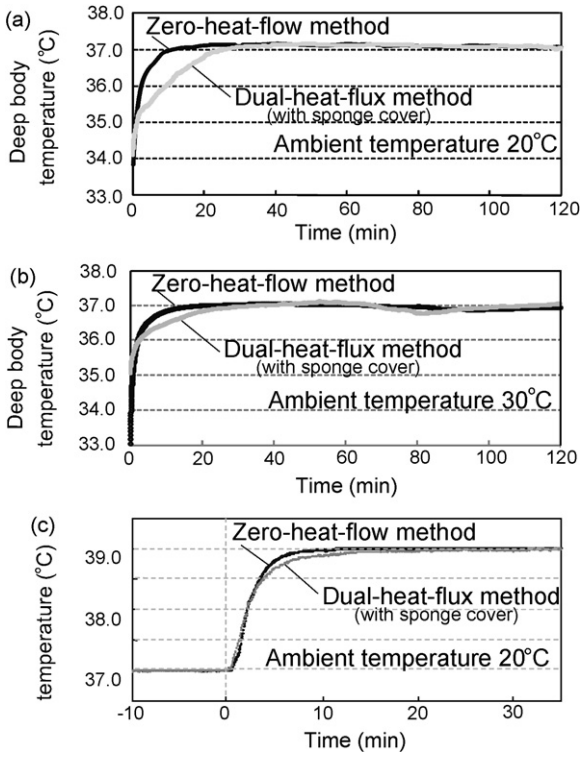

Fig. 4. The initial responses and step responses of the dual-heat-flux and zero-heat-flow methods. The initial responses of the deep body temperature in the anterior temporal region at the ambient temperature of 20 °C (a) and 30 °C (b) were compared between the dual-heat-flux method and the zero-heat-flow method. (c) The step responses due to the rapid changes in the core temperature (2.0 °C/10 min) in the simulation experiment were compared between the dual-heat-flux method and the zero-heat-flow method.

3.3. Initial response

Fig. 4(a) and (b) shows representative data for the deep body temperature using the zero-heat-flow and dual-heat-flux methods in the anterior temporal region at the ambient temperatures of 20 °C and 30 °C. The initial response time, measured from the time when the probe is placed on the body surface to the time when the first thermal equilibrium is achieved, was approximately 15–20 min for the zero-heat-flow method and approximately 30–40 min for the dual-heat-flux method. Consequently, the delay in the initial response with the dual-heat-flux method was approximately twice that with the conventional zero-heat-flow method.

3.4. Step responses to changes in the deep temperature

The results of the step responses to the rapid changes in the deep temperature (at a rate higher than 0.2 °C/min) in the simulation experiment are shown in Fig. 4(c). Although there

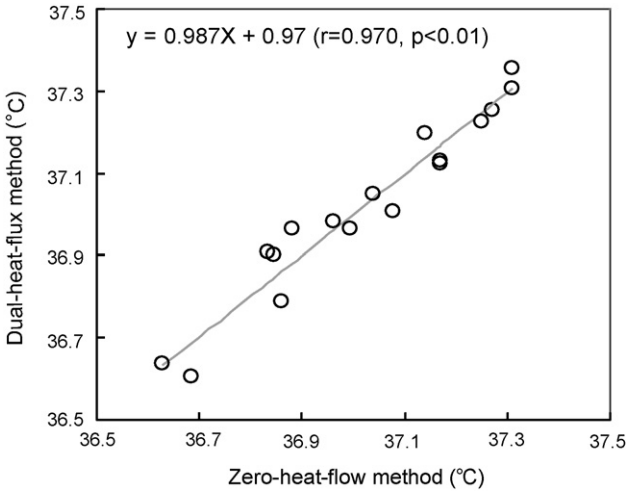

Fig. 5. The linear correlation of the deep temperatures measured in the bilateral anterior temporal regions of 17 young subjects using the dual-heat-flux and zero-heat-flow methods. The head deep temperature measured using the dual-heat-flux method (y-axis) was significantly correlated ($p < 0.001$) with the temperature measured using the zero-heat-flow method (x-axis).

seemed to be a slight delay in the measurement with our dual-heat-flux system when compared with the zero-heat-flow method, both these methods exhibited good traceability for the rapid temperature change after the attainment of thermal equilibrium.

3.5. The relationship between the head deep temperatures measured using the zero-heat-flow method and those measured using the dual-heat-flux method

Fig. 5 shows the relationship between the head deep temperatures measured in 17 healthy subjects using the dual-heat-flux method and those measured using the zero-heat-flow method. The head deep temperatures measured by the 2 methods were significantly correlated with each other ($r = 0.970$, $p < 0.001$). The mean transcutaneously measured deep body temperature determined using the zero-heat-flow method was 37.02 °C and that determined using the dual-heat-flux method was 37.08 °C.

4. Discussion

We developed a new noninvasive technique for the measurement of the deep body temperature, and compared it with the zero-heat-flow method, which is now most widely used in cardiac surgery. The comparison of the deep head temperatures measured in 17 healthy subjects in this study revealed that the accuracies of the conventional zero-heat-flow method and our dual-heat-flux method were comparable.

Because many comparative studies of zero-heat-flow data and rectal temperatures, which have been widely used as indices of core body temperature, have already been reported, we compared the new dual-heat-flux method only with the conventional zero-heat-flow method for the measurement of deep head temperature in the present study. With the zero-heat-flow probe, the temperature measured at the upper sternum was found to be 0.2–0.4 °C lower than that measured at the rectum [15]. Togawa et al. [16] reported that the mean deep temperature measured with the zero-heat-flow probe at the occipital region was 36.68 °C, while the mean rectal temperature was 36.78 °C in 15 healthy subjects. Accordingly, the deep head temperature measured by the dual-heat-flux method seems to be approximately 0.0–0.5 °C lower than the rectal temperature though it did not compare directly with the rectal temperature in the present study.

It takes approximately 15–20 min to reach the final equilibrium temperature even by the zero-heat-flow method, which involves the use of a servocontrolled electrical heater (Fig. 4(a) and (b)). Approximately 30–40 min after the application of the probe to the head at an ambient temperature of 20 °C, the final equilibrium temperature, which was within 0.1 °C of that measured with the zero-heat-flow method, was obtained by the dual-heat-flux method. Although the initial response time could be considered to be shortened by pre-warming the probe, attainment of the equilibrium temperature still required a long time when the body surface was cold (data not shown). The slow initial responses seem to inherently express the principle of the dual-heat-flux method, i.e., the probe does not have a heater. Thus, some improvements such as replacement of copper materials by aluminum may be useful to reduce the thermal inertia of the probe. The response time after obtaining the initial thermal equilibrium state, however, does not seem to correlate with the initial response time. In the rapid response experiment of the simulation, not only the zero-heat-flow method but also the dual-heat-flux method exhibited good traceability for the rapid temperature change after the attainment of thermal equilibrium (Fig. 4(c)). Under physiological conditions, a rapid change in the core body temperature such as 2.0 °C in 10 min cannot be observed because of the large thermal inertia of the human body. In addition, Fox and Solman [11] reported an experiment in which a continuous increase of 1.5 °C in the core temperature in 80 min was induced at the onset of fever by the intravenous injection of an endogenous pyrogen; they observed that the sternum core temperature measured by the zero-heat-flow method did not lag behind the auditory canal temperature and intestinal temperature measured by the radio pill. Therefore, under physiological conditions, the dual-heat-flux method as well as the zero-heat-flow method seems to exhibit adequate traceability for the measurement of the core body temperature after the thermal equilibrium state is achieved.

In the zero-heat-flow method with a servocontrolled heater, ambient temperature changes do not affect the measurements of the head or torso core temperature [11]. In our dual-heat-flux method, however, the estimated thermal resistance ratio K of the probe changed according to the changes in the ambient temperature. In the simulation experiments, the estimated K values were found to be sensitive to the ambient temperature, and the K values were 2.5 and 3.0 at the ambient temperatures of 20 °C and 30 °C, respectively. Furthermore, when the probe was covered with a urethane sponge to avoid the influence from the air flow, the estimated K value increased to 4.0 at an ambient temperature of 20 °C (Fig. 3(a)). When the core water temperatures were calculated using each estimated K value in each simulation experiment, all calculated deep temperatures were within 0.1 °C from the set value (37.00 °C) (Fig. 3(b)). We concluded that similar to the case of the zero-heat-flow method, measurement of the deep temperature by the dual-heat-flux method is not affected by changes in the ambient temperature if the K value is adjusted according to the ambient temperature.

The thermal resistance ratio K was not affected by the rubber sheet thickness in the range of 0–10 mm, but it was sensitive to changes in the ambient temperature and the presence of a sponge cover (Fig. 3(a)). At an ambient temperature of 20 °C, the estimated thermal resistance ratio K in the simulation experiment was 2.5 and therefore larger than 1.86, which is the ratio of the lengths of the 2 flux channels of the heat insulator in the probe. In addition, when the probe was covered with a urethane sponge, the K value was considerably larger, i.e., 4.0. The actual

heat conduction in the probe consists of not only the vertical flow from the bottom (IC_1) to the top (IC_3) but also the horizontal flow from the center to the sides. The horizontal flow may increase the heat current from IC_2 to IC_4. The magnitude and directionality of the heat conduction in the material are determined by the local temperature gradient in the material, known as the Fourier's law. Therefore, when the horizontal temperature gradient increases when compared with the vertical temperature gradient in the probe, the relative ratio of the vertical heat flow to the total heat flow at the central portion of the probe will decrease. As a result, the relative thermal resistance in the vertical direction at the central portion of the probe will increase, while that at the periphery will decrease. Consequently, the augmentation of K value in our simulation experiment suggested that when the ambient temperature increases or the probe is covered with a urethane sponge, the horizontal temperature gradient seems to increase in comparison to the vertical temperature gradient in the probe.

The dermis of the skin has blood vessels; therefore, conduction and convection influence heat flux. However, the circulation volume of the blood in these tissues is insufficient as compared to that in the isothermal tissue of the deep body. The role of thermal conduction in thermal migration in the skin and subcutaneous fat is still considered to be significant. Therefore, in the simulation experiment, which was conducted as described by Nemoto and Togawa [14], we adopted rubber as a model for the skin and hypodermis tissues, because the thermal conductivity of the rubber sheet was $0.17\,W\,m^{-1}\,K^{-1}$, which is similar to those of skin and subcutaneous fat, where a temperature gradient is produced from the body core to the skin surface. In our simulation experiment, the thermal resistance ratio K was not affected by the thickness of the rubber sheet in the range of 0–10 mm (Fig. 3(a)). These results suggested that the accurate estimation of the deep body temperature by the dual-heat-flux method might be feasible when the sum of the thickness of the skin and that of subcutaneous fat is less than 10 mm. This sum is approximately constant in the forehead, temporal region, and preauricular region, and the mean thickness of these tissues is 6.7 mm in the adult preauricular region [17]; thus, the head is a preferable measurement location if we wish to attain accurate measurement of the deep body temperature by the dual-heat-flux method.

Finally, the results of our present study suggested that our dual-heat-flux method is promising for the long-term and accurate portable monitoring of the deep body temperature under unconstrained conditions.

Acknowledgments

This study was supported in part by grants to K. Kitamura (Grant-in-Aid for Scientific Research (C) no. 21500681) and to T. Nemoto (Grant-in-Aid for Scientific Research (C) no. 21500405).

Conflict of interest statement

All authors disclose any financial and personal relationships with other people or organisations that could inappropriately influence (bias) their work.

References

[1] Gal R, Slezak M, Zimova I, Cundrle I, Ondraskova H, Seidlova D. Therapeutic hypothermia after out-of-hospital cardiac arrest with the target temperature 34–35 degrees C. Bratisl Lek Listy 2009;110:222–5.
[2] Oddo M, Schaller MD, Feihl F, Ribordy V, Liaudet L. From evidence to clinical practice: effective implementation of therapeutic hypothermia to improve patient outcome after cardiac arrest. Crit Care Med 2006;34:1865–73.
[3] Rowland T, Garrison A, Pober D. Determinants of endurance exercise capacity in the heat in prepubertal boys. Int J Sports Med 2007;28:26–32.
[4] Chambers CD. Risks of hyperthermia associated with hot tub or spa use by pregnant women. Birth Defects Res A Clin Mol Teratol 2006;76:569–73.
[5] Stanger R, Colyvas K, Cassey JG, Robinson IA, Armstrong P. Predicting the efficacy of convection warming in anaesthetized children. Br J Anaesth 2009;103:275–82.
[6] Wallace CT, Marks Jr WE, Adkins WY, Mahaffey JE. Perforation of the tympanic membrane, a complication of tympanic thermometry during anesthesia. Anesthesiology 1974;41:290–1.
[7] Tabor MW, Blaho DM, Schriver WR. Tympanic membrane perforation: complication of tympanic thermometry during general anesthesia. Oral Surg Oral Med Oral Pathol 1981;51:581–3.
[8] Vale RJ. Monitoring temperature during anesthesia. Int Anesthesiol Clin 1981;19:61–83.
[9] Lipkin M, Hardy JD. Measurement of some thermal properties of human tissue. J Appl Physiol 1954;7:212–7.
[10] Fox RH, Solman AJ. A new technique for monitoring the deep body temperature in man from the intact skin surface. J Physiol 1971;212:8P–10P.
[11] Fox RH, Solman AJ, Issacs R, Fry AJ, MacDonald IC. A new method for monitoring deep body temperature from the skin surface. Clin Sci 1973;44:81–6.
[12] Tsuji T. Patient monitoring during and after open heart surgery by an improved deep body thermometer. Med Prog Technol 1987;12:25–38.
[13] Togawa T, Nemoto T, Tsuji T, Suma K. Deep temperature monitoring in intensive care. Resuscitation 1979;7:53–7.
[14] Nemoto T, Togawa T. Improved probe for a deep body thermometer. Med Biol Eng Comput 1988;26:456–9.
[15] Ball SG, Chalmers McM, Morgan AG, Solman AJ, Losowsky MS. A clinical appraisal of transcutaneous deep body temperature. Biomedicine 1973;18:290–4.
[16] Togawa T, Nemoto T, Yamazaki T, Kobayshi T. A modified internal temperature measurement device. Med Biol Eng 1976;14:361–4.
[17] Hwang K, Han JY, Kim DJ. Dermofat graft in deep nasolabial fold and facial rhytidectomy. Aesthetic Plast Surg 2003;27:254–7.